Journal of Cellular Biochemistry 93:1084–1098 (2004)

Gene Positional Changes Relative to the Nuclear Substructure During Carbon Tetrachloride-Induced Hepatic Fibrosis in Rats

Apolinar Maya-Mendoza,[1,2] Rolando Hernández-Muñoz,[3] Patricio Gariglio,[2] and Armando Aranda-Anzaldo[1]*

[1]Laboratorio de Biología Molecular, Facultad de Medicina, Universidad Autónoma del Estado de México, Apdo. Postal 428, C.P. 50000, Toluca, Edo. Méx., México
[2]Departamento de Genética y Biología Molecular, CINVESTAV-IPN, Apdo. Postal 14-740, 07000 D.F., México
[3]Departamento de Biología Celular, Instituto de Fisiología Celular, UNAM, 04510, D.F., México

Abstract In the interphase nucleus the DNA of higher eukaryotes is organized in loops anchored to a substructure known as the nuclear matrix (NM). The topological relationship between gene sequences located in the DNA loops and the NM appears to be very important for nuclear physiology because processes such as replication, transcription, and processing of primary transcripts occur at macromolecular complexes located at discrete sites upon the NM. Mammalian hepatocytes rarely divide but preserve a proliferating capacity that is displayed in vivo after specific stimulus. We have previously shown that transient changes in the relative position of specific genes to the NM occur during the process of liver regeneration after partial ablation of the liver, but also that such changes correlate with the replicating status of the cells. Moreover, since chronic exposure to carbon tetrachloride (CCl_4) leads to bouts of hepatocyte damage and regeneration, and eventually to non-reversible liver fibrosis in the rat, we used this animal model in order to explore if genes that show differential activity in the liver change or modify their relative position to the NM during the process of liver fibrosis induction. We found that changes in the relative position of specific genes to the NM occur during the chronic administration of CCl_4, but also that such changes correlate with the proliferating status of the hepatocytes that goes from quiescence to regeneration to replicative senescence along the course of CCl_4-induced liver fibrosis, indicating that specific configurations in the higher-order DNA structure underlie the stages of progression towards liver fibrosis. J. Cell. Biochem. 93: 1084–1098, 2004.

Key words: DNA loops; DNA replication; DNA topology; liver fibrosis; nuclear matrix

During the interphase the DNA of higher eukaryotes is organized in loops anchored to a nuclear substructure commonly known as the nuclear matrix (NM). Such loops are topologically constrained and supercoiled [Cook et al., 1976; Roti-Roti et al., 1993; Nickerson, 2001]. The DNA loops are attached to the proteinaceous substructure by means of non-coding sequences known as matrix attachment regions (MARs) [Razin, 2001]. Fundamental processes of nuclear physiology, such as replication, transcription, and processing of primary transcripts seem to occur at macromolecular complexes located at discrete sites upon the NM [Berezney et al., 1995; Jackson and Cook, 1995; Cook, 1999]. The topological relationship between gene sequences located in the DNA loops and the NM appears to be very important for appropriate nuclear physiology [Stein et al., 1995]. Indeed, correct repair of DNA damage must include recovery of both the double helix integrity and the complex, three-dimensional DNA topology, otherwise the cell will not survive [Aranda-Anzaldo and Dent, 1997; Aranda-Anzaldo et al., 1999]. The hepatocytes

Grant sponsor: CONACYT, México (to A.A.-A.); Grant number: 33539-N.

*Correspondence to: Armando Aranda-Anzaldo, MD, PhD, Laboratorio de Biología Molecular, Facultad de Medicina, UAEMéx. Apartado Postal 428, C.P. 50000 Toluca, Edo. Méx., México. E-mail: aaa@uaemex.mx

Received 30 March 2004; Accepted 9 July 2004

DOI 10.1002/jcb.20264

display a proliferating capacity in vivo under specific stimulus. We have previously shown that transient changes in the relative position of specific genes to the NM occur during the process of liver regeneration after partial hepatectomy, but also that such changes correlate with the replicating status of the cells [Maya-Mendoza et al., 2003]. Moreover, chronic administration of carbon tetrachloride (CCl_4) in rats causes repeated bouts of hepatocyte necrosis, inflammation, and regeneration, eventually leading to extensive hepatic fibrosis and the establishment of micronodular cirrhosis [Panduro et al., 1988; Hernández-Muñoz et al., 1997]. We have used this animal model coupled to a PCR-based method for mapping the position of specific DNA sequences relative to the NM [Maya-Mendoza and Aranda-Anzaldo, 2003] in order to determine whether the topological relationships between specific DNA sequences and the nuclear substructure remain invariant or change after the critical nuclear transitions associated with cell proliferation and tissue regeneration during the chronic administration of CCl_4. We provide evidence that changes in the relative position of specific genes to the NM do occur, but also that most of such changes correlate with the replicating status of the hepatocytes that shift from quiescence to replication and eventually to replicative senescence in the course of CCl_4-induced liver fibrosis.

MATERIALS AND METHODS

CCl_4-Induced Liver Injury and Fibrosis

Procedures involving animals were done following the Institutional Guide for Ethical Animal Experimentation (National Autonomous University of Mexico). Male Wistar rats with an initial weight of 100–110 g were used. Rats were injected intraperitoneally with CCl_4 at 0.4 g/kg in a 150 μl volume (25 μl of CCl_4 stock plus 125 μl of vegetable oil) three-times per week. Animals were administered CCl_4 until 8 weeks. The liver of each treated animal was examined and further processed at 1, 2, 4, and 8 weeks after treatment (animals were sacrificed using ether anesthesia 24 h after the last CCl_4 injection). This protocol for liver fibrosis induction did not impair normal weight gain and growth in the treated animals, yet the fibrosis induction is reversible during the first 4 weeks of treatment but by 8 weeks of CCl_4 treatment the process becomes irreversible [Ehrinpreis et al., 1980; Panduro et al., 1988; Hernández-Muñoz et al., 1990]. Appropriate groups of control animals injected with vegetable oil were run simultaneously. The experimental results were very similar among the different control groups.

Hepatocytes

Previous to the hepatocyte isolation the livers were washed in situ by perfusion with PBS without Ca^{2+} and Mg^{2+} at 37°C for 5 min at 15 ml/min; next the tissue was perfused with a solution of collagenase IV, Sigma (0.025% collagenase with 0.075% of $CaCl_2$ in Hepes buffer pH 7.6) for 15 min. The rest of the hepatocyte isolation was carried out as described [Freshney, 1994].

Preparation of Nucleoids

The DNA loops plus the NM constitute a "nucleoid." Freshly isolated and washed hepatocytes are suspended in ice-cold PBS without Ca^{2+} and Mg^{2+} (PBS-A). Aliquots of 50 μl containing 3.5×10^5 cells are gently mixed with 150 μl of a lysis solution containing 2.6 M NaCl, 1.3 mM EDTA, 2.6 mM Tris, 0.6 % Triton X-100, pH 8.0 and then further processed to isolate nucleoids as previously described [Maya-Mendoza and Aranda-Anzaldo, 2003].

DNase I Digestion of Nucleoid Samples

The washed nucleoids are pooled (2×10^6 nucleoids in 1.2 ml of PBS-A) and mixed with DNase I digestion buffer: 10 mM $MgCl_2$, 0.1 mM dithiothreitol, 50 mM Tris at pH 7.2 (usually 5 ml of digestion buffer for each 1.2 ml of nucleoid suspension). Digestions were carried out at 37°C with 0.5 U/ml DNase I (Sigma-Aldrich, St. Louis, MO). Each digestion time-point aliquot contains 3.5×10^5 nucleoids. Enzyme digestion was stopped by adding enough stop buffer (0.2 M EDTA and 10 mM Tris at pH 7.5) to achieve an EDTA concentration of 30 mM. After digestion with DNase I, the NM-bound DNA was determined by spectrometry on aliquots of partially digested nucleoid samples that were washed and further handled as previously described [Maya-Mendoza and Aranda-Anzaldo, 2003]. The final nucleoid pellet is re-suspended in double distilled-H_2O (100–200 μl) to be used directly as template for PCR.

PCR Amplification

Four hundred nanogram of NM-bound DNA were used as template for PCR. Standard PCR was carried out using Taq Polymerase (GIBCO-BRL, Life Technologies, Paisley, UK). Following the appropriate controls previously described [Maya-Mendoza and Aranda-Anzaldo, 2003], the same amplification program was used for all pairs of primers (25 pmol): 94°C for 5 min, 35× (94°C for 45 s, 56°C for 30 s, and 72°C for 1 min), and final extension at 72°C for 10 min. The identity of amplified sequences was confirmed by restriction analysis. Amplified PCR products were electrophoresed on 2% agarose gels and visualized using ethidium bromide staining, recorded and analyzed using a Eastman Kodak 1D Image Analysis Software 3.5 system (Rochester, NY).

Genomic DNA Primers

For the positional mapping of specific gene sequences relative to the NM we used the following primers: Rat β-actin (Accession numbers: V01217; J00691); Sen. 5′-CGTAAAGACCTCTATGCCA. Ant. 5′-AGCCATGCCAAATGTGTCAT. Amplicon size: 473 bp. Location: exon 5-intron 5-exon 6. Chromosome: 12q11. Universal β-actin (Accession number: M10277); Sen. 5′-AACACCCCAGCCATGTACG. Ant. 5′-ATGTCACGCACGATTTCCC. Amplicon size: 254 bp. Location: exon 4. Chromosome: 12q11. Rat albumin gene (Accession number: M16825); Sen. 5′-GGGATTTAGTTAAACAACTT. Ant. 5′-AAAGGTTACCCACTTCATTG. Amplicon size: 206 bp. Location: promoter/exon1. Chromosome 14p22. Rat alpha-fetoprotein gene (Accession number: J02816); Sen. 5′-ACCCATGCATCTGTGACATA. Ant. 5′-AGTAAAATGCATGTTGCCTG. Amplicon size: 252 bp. Location: 5′ flanking region. Chromosome: 14p21. Rat *c-myc* gene (Accession number: Y00396); Sen. 5′-TATAATCCGGGGGTCTGCGC. Ant. 5′-CCCTCTGTCTCTCGCTGGAA. Amplicon size: 227 bp. Location: untranslated promoter. Chromosome: 7q33. Rat collagen type I alpha-1 gene (Accession number: J04464); Sen. 5′-CATACCTGGGCCCACACCAT. Ant. 5′-CTTGCACTTTCCTTCTGGGA. Amplicon size: 261 bp. Location: 5′ flanking region. Chromosome: 11. Rat inositol trisphosphate receptor subtype 3 (IP3R3) mRNA, (Complete cDNAs, Accession number: L06096); Sen 5′-GGTGAGCGGCGAGGGCGAGG. Ant 5′-GCAGTTCTGCACGTCCACGA. Amplicon size: 480 bp. Location: nucleotides 7961–8136 in mRNA. Chromosome: 20.

RT-PCR

Total RNA of isolated hepatocytes was obtained using RNAqueous™-4PCR (Ambion Inc., Austin, TX). All RNA samples were quantified and normalized using spectrophotometric methods. Double-stranded cDNA was synthesized from extracted RNA using SUPERSCRIPT II (GIBCO-BRL) and random primers according to the manufacturer's protocol. Reverse transcription was performed using 500 ng of RNA. Different amplification programs were used depending on the pair of primers (25 pmol): 94°C for 5 min, 30–32× (94°C for 45 s, 56–60°C for 30 s, and 72°C for 1 min), and final extension at 72°C for 10 min (specifically: *β-actin*: 56°C, 30 cycles; *IP3R3*: 56°C, 32 cycles; *ALB*: 58°C, 30 cycles; *AFP*: 60°C, 32 cycles; *c-myc*: 60°C, 30 cycles; *COL1A1*: 60°C, 30 cycles).

RT Primers

Rat gene encoding cytoplasmic β-actin (Accession numbers: V01217, J00691); Sen. 5′-CGTAAAGACCTCTATGCCAA. Ant. 5′-AGCCATGCCAAATGTGTCAT. Amplicon size: 349 bp. Location: exon 5-exon 6. Rat inositol trisphosphate receptor subtype 3 (IP3R3) mRNA (Complete cDNAs Accession number: L06096); Sen 5′-GGTGAGCGGCGAGGGCGAGG. Ant 5′-GCAGTTCTGCACGTCCACGA. Amplicon size: 175 bp. Location: nucleotides 7961–8136 in mRNA. Rat Albumin (Alb), mRNA (Accession number: NM_134326); Sen 5′-ATACACCCAGAAAGCACCTC. Ant 5′-CACGAATTGTGCGAATGTCAC. Amplicon size: 436 bp. Location: nucleotides 1301–1737 in mRNA. Rat alpha-fetoprotein (AFP), mRNA (Accession number: NM_012493); Sen 5′-CAGTGAGGAGAAACGGTCCG. Ant 5′-ATGGTCTGTAGGGCTCGGCC. Amplicon size: 252 bp. Location: nucleotides 1421–1673 in mRNA. Rat v-myc avian myelocytomatosis viral oncogene homologue (*c-myc*), mRNA (Accession number: NM_012603); Sen 5′-AGTGCATTGATCCCTCAGTGGTCTTTCCCTA. Ant 5′-CAGCTCGGTTCCTCCTCTGACGTTCCAAGACGTT. Amplicon size: 548 bp. Location: nucleotides 976–1524 in mRNA. Rat collagen type I alpha-1 gene (*COL1A1*), exon 1 (Accession numbers: XM_109776, J04464); Sen 5′ - GAGTGAGGCCACGCATCAGCCGAAGCTAAC. Ant 5′-AAGAGGAGCAGGAGCCGGAGG-

TCCACAAAG. Amplicon size: 111 bp. Location: nucleotides 33–144 in mRNA.

RESULTS

Nucleoids (NM plus attached DNA loops) prepared from freshly isolated hepatocytes from either control or CCl_4-treated rats were subjected to our protocol for mapping the relative position of specific gene sequences to the NM by PCR on NM-bound templates [Maya-Mendoza and Aranda-Anzaldo, 2003]. The method involves the progressive detachment of DNA from the nuclear substructure by digestion with a carefully adjusted concentration of DNase I. Under our assay conditions resistance to detachment is directly proportional to the DNA sequence proximity to the anchoring point on the NM [Razin et al., 1995; Maya-Mendoza and Aranda-Anzaldo, 2003]. However, for the mapping protocol to work it is necessary to satisfy two basic conditions: (1) the loop DNA must be equally accessible to the endonuclease (except for those regions close to the nuclear substructure framework). This condition is achieved by high-salt extraction during nucleoid preparation that removes most histones and other chromatin proteins, therefore, the nuclear DNA is not anymore organized into chromatin as such, and yet the DNA loops remain anchored to the NM and supercoiled [Cook et al., 1976; Roti-Roti et al., 1993; Aranda-Anzaldo and Dent, 1997]. (2) The nuclease should cut all DNA sequences with an equal probability otherwise, the relative distance between the DNA sequence under study and the NM attachment site can't be actually established [Razin et al., 1995; Razin, 2001]. The second condition is achieved by using a non-specific nuclease such as DNase I. Therefore, the relative resistance of a given DNA sequence to detachment from the matrix by DNase I is just a statistical phenomenon resulting from the average position of the sequence relative to the NM attachment point, and it reflects no intrinsic resistance of a given DNA sequence to the endonuclease. Detailed descriptions of our experimental procedures and conditions have already been published [Maya-Mendoza and Aranda-Anzaldo, 2003; Maya-Mendoza et al., 2003].

Differential Kinetics of Nucleoid-DNA Digestion During Liver Fibrosis Induction

We determined the kinetics of DNA digestion with a low concentration of DNase I in nucleoids prepared from rat hepatocytes corresponding to different weeks of CCl_4 treatment (Fig. 1). Samples from 1 to 4 weeks of treatment show a faster kinetics of DNA digestion than the non-treated controls. In samples from 2 and 4 weeks of CCl_4 treatment the residual DNA attached to the matrix after 60 min of digestion is less than half the value of the control sample. Yet, at 8 weeks of CCl_4 treatment, the kinetics of DNA digestion becomes slower than the control and a larger fraction of bulk DNA remains attached to the NM after 60 min of digestion with DNase I.

Amplification of Specific Gene-Target Sequences on NM-Bound Templates

We chose specific sequences belonging to six different genes for mapping their relative position to the NM. Four genes: *β-actin*, *c-myc*, collagen type 1 (*COL1A1*), and inositol 1,4,5-trisphosphate receptor type 3 (*IP3R3*), are located in four different rat chromosomes, while two other genes: albumin (*ALB*) and alpha-fetoprotein (*AFP*), are located at 15 kbp of each other in the multi-locus region of the albumin-gene family cluster in the long arm of the chromosome 14 of the rat [Lazarevich, 2000]. The *β-actin* is an example of constitutive gene since the β-actin protein is a major constituent of most cell types. The gene *c-myc* is poorly expressed in quiescent hepatocytes but quickly increases its transcription under conditions that stimulate hepatocyte proliferation [Morello et al., 1990]. *COL1A1* is highly expressed in liver tissue undergoing CCl_4-induced fibrosis [Panduro et al., 1988]. *IP3R3* had been reported as non-expressed in normal liver [Blondel et al., 1993], but it has been shown that after chronic exposure to CCl_4, a mildly enhanced expression of this gene is detected in liver-homogenate samples [Dufour et al., 1999]. *ALB* is highly expressed in rat adult liver, and there is a relative increase of *ALB* transcription during the 3rd–7th week of treatment with CCl_4 [Lazarevich, 2000]. *AFP* is repressed in rat adult liver and it becomes active in the course of acute and chronic intoxication by CCl_4 [Panduro et al., 1988; Lazarevich, 2000]. Specific amplicons were obtained by PCR amplification on NM-bound templates after progressive DNase I digestion of the corresponding nucleoids (Fig. 2). It is very important to stress that in our mapping protocol the actual intensity of the amplicon signal at each particular DNase I digestion time is non-relevant because the PCR is not

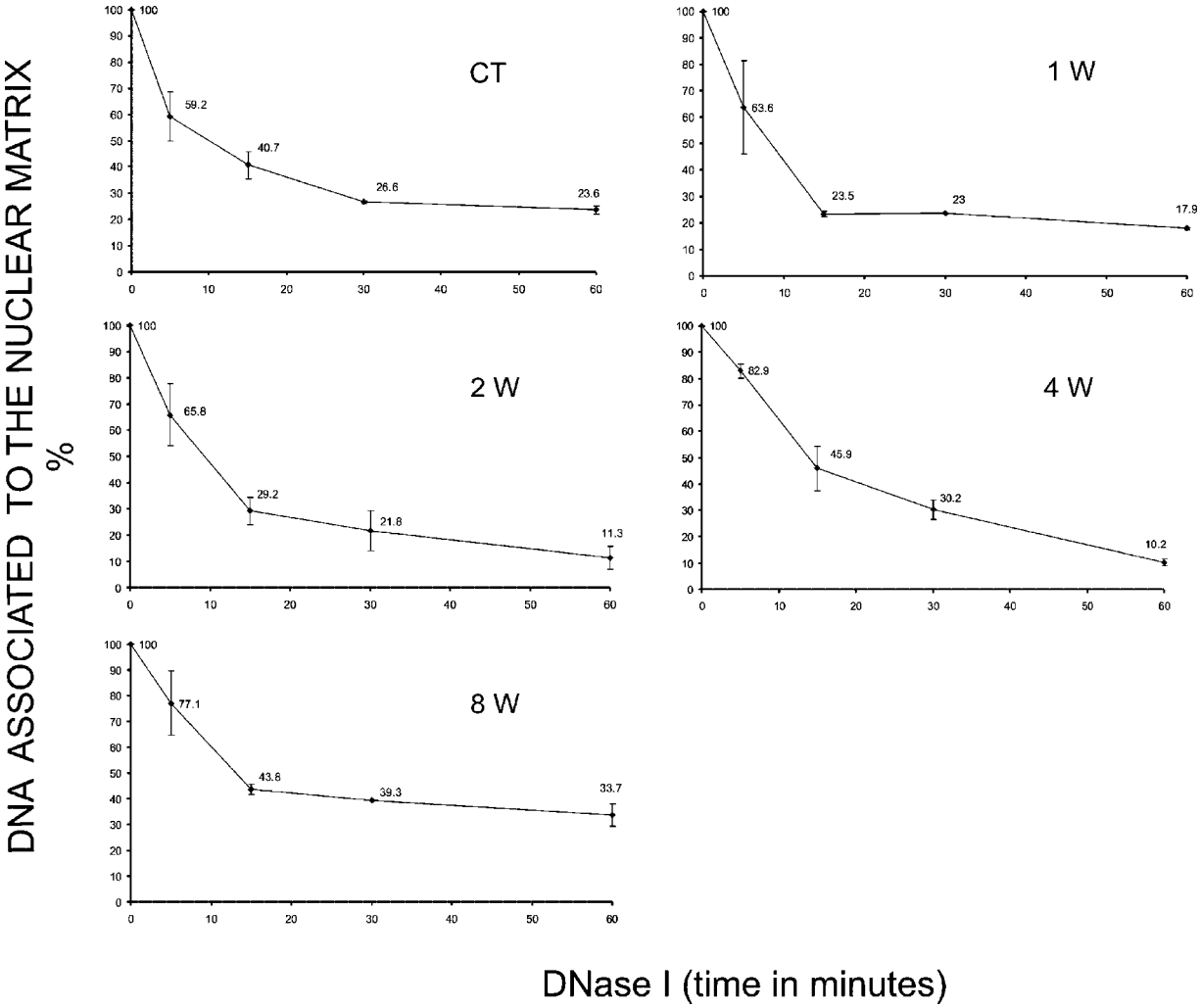

Fig. 1. Kinetics of DNA digestion in nucleoids from hepatocytes at different times of treatment with carbon tetrachloride (CCl_4). Nucleoid samples were digested with DNase I (0.5 U/ml) and further processed as described in ''Materials and Methods.'' The residual amount of nuclear matrix (NM)-bound DNA was quantified by spectrometry. Each time-point value is the average of separate DNA digestion curves of nucleoids obtained from independent animals treated in a similar way. The S.D. was calculated from the pooled values of independent experiments corresponding to each digestion time-point. Non-CCl_4 treated control (CT), n = 5 rats. CCl_4 treated samples: 1, 2, 8 weeks, n = 3 rats; 4 weeks, n = 4 rats, for each DNA digestion curve corresponding to each particular time of CCl_4 treatment.

quantitative. The amplicon signals are scored either as positive or negative, based on whether they are detected or not by a digital image analysis system, since we are monitoring the average DNA loop arrangement in a large number of nucleoids from hepatocytes and so the observed degree of resistance to digestion of a given DNA sequence corresponds to its average across the large nucleoid population analyzed. For example: the β-actin amplicon is observed in samples from control hepatocyte nucleoids at 0, 5, and 15 min of DNA digestion, but it is absent in samples digested for 30 and 60 min. Thus, the critical parameter is whether a particular DNA sequence can be amplified or not after a given time of nucleoid-DNA digestion with DNase I. Therefore, in nucleoids of hepatocytes isolated from rats after 1 week and up to 8 weeks of CCl_4 treatment the β-actin amplicon is detected up to 30 min of DNA digestion but is completely absent in samples digested for 60 min (Fig. 2).

Genes Become Closer to the NM During the Regenerative Phase of Liver Fibrosis

The PCR-amplification results (Fig. 2) are calibrated using as a gauge the percentage of total DNA remaining associated with the NM at each digestion time and according to the stage-specific kinetics of nucleoid-DNA digestion (Fig. 1). This kind of analysis establishes

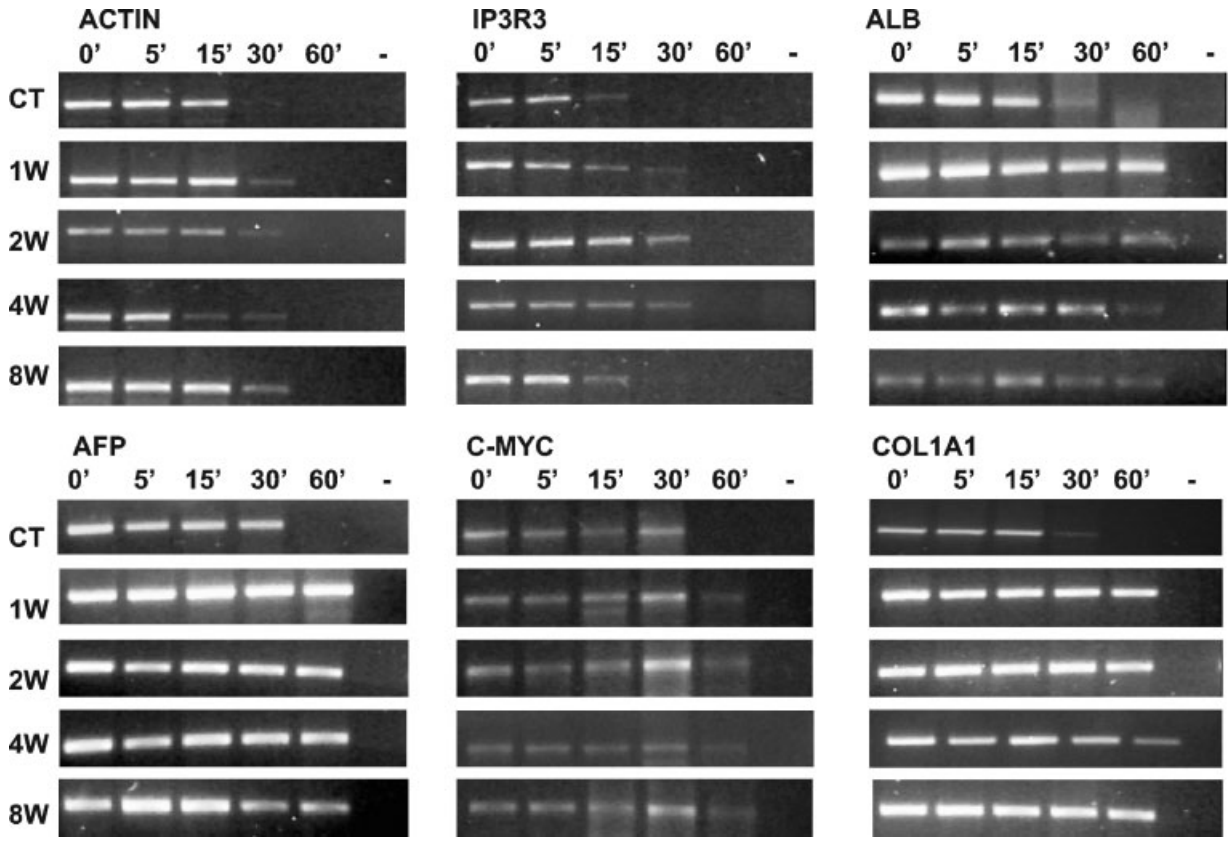

Fig. 2. Specific PCR-amplification products corresponding to the target sequences of the six genes (*β-actin*, *IP3R3*, *ALB*, *AFP*, *c-myc*, and *COL1A1*) whose position relative to NM was mapped in nucleoids from hepatocytes undergoing CCl_4-treatment. Nucleoids from isolated hepatocytes were treated with DNase I (0.5 U/ml) for 0, 5, 15, 30, and 60 min and further processed for direct PCR-amplification of the target sequences on NM-bound templates (see ''Materials and Methods''). The presence of the target sequence in the residual NM-bound DNA of the partially digested samples was scored as positive if the amplicon was detected by the Kodak 1D Image Analysis Software version 3.5. CT = non-CCl_4 treated control. CCl_4-treated samples: 1, 2, 4, 8 weeks. The amplicon patterns were consistently reproduced in separate experiments with samples from independent animals (CT, n = 5 rats; CCl_4-treated samples 1, 2, 8 weeks, n = 3 rats; 4 weeks, n = 4 rats).

average positional windows relative to the NM for the mapped gene sequences. The upper values on each window correspond to the percentage of total DNA associated with the NM at which each specific amplicon was last detected. The lower values correspond to the percentage of total DNA associated with the NM at which each specific amplicon was not detected anymore. Hence, the specific DNA sequence corresponding to each amplicon is expected to be actually located within the interval defined by such values (Fig. 3). Therefore, the *β-actin* gene becomes progressively closer to the NM during the chemical induction of liver fibrosis, reaching it closest position at 4 weeks of CCl_4 treatment but then becomes further remote from the NM at 8 weeks of treatment. Indeed, all genes studied became proximal to the NM within 1–4 weeks of CCl_4 treatment, but they withdraw to a more distal position by 8 weeks of CCl_4 treatment. This is well illustrated by the genes *β-actin* and *IP3R3* whose positional windows at 8 weeks of CCl_4 treatment were clearly defined (Figs. 2 and 3) in spite of the very slow kinetics of nucleoid-DNA digestion that left more than 33% of total DNA attached to the nuclear substructure even after 60 min of DNAse I treatment (Fig. 1). This fact precluded the formal extinction of the amplification signals for *ALB*, *AFP*, *c-myc*, and *COL1A1*, in the nucleoid samples from livers treated for 8 weeks with CCl_4, since in all cases digestion curves were carried out only up to 60 min (Figs. 1–3).

Gene Position Relative to the NM and the Gene Expression Level

Several reports indicate a correlation between proximal position or actual attachment

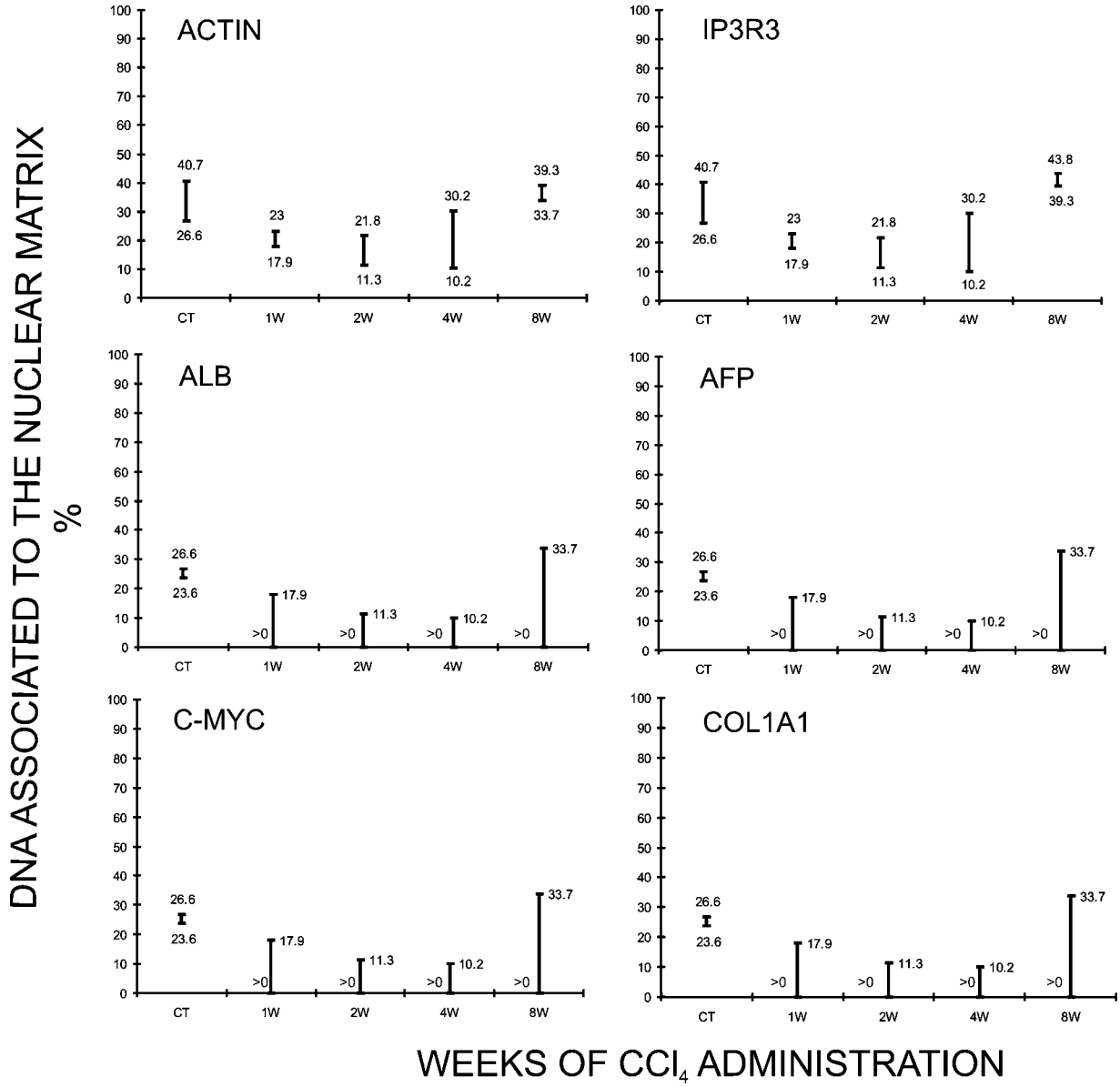

Fig. 3. Positional windows relative to the NM for the specific gene sequences mapped in nucleoid samples at different times of CCl_4-treatment. The upper values on each bar correspond to percentage of total DNA associated with the NM at which each specific amplicon was last detected. The lower values correspond to percentage of total DNA associated with the NM at which each specific amplicon was not detected anymore. Hence, the specific DNA sequence corresponding to each amplicon is expected to be actually located within the interval defined by such values. Note that in some cases it was not possible to define the lower boundary value because all nucleoid-DNA digestions were carried out up to 60 min (Fig. 1), and for some genes such as *ALB, AFP, c-myc,* and *COL1A1* the specific target sequence was amplified and detected up to the very last point of the nucleoid-DNA digestion curve since the nucleoid-DNA digestion curves depicted in Figure 1 were used as gauges for establishing such intervals based on the amplification data shown in Figure 2. Positional windows lacking the lower boundary are labeled >0 to indicate that the specific gene sequence must be actually located between the specific window upper-boundary value and a greater than zero amount of residual NM-bound DNA.

of a given gene to the nuclear substructure and its transcription [Cook et al., 1982; Robinson et al., 1982; Ciejek et al., 1983; Small et al., 1985; Dalton et al., 1986; Ramana-Murty et al., 1988]. We did standard RT-PCR experiments in order to assess the expression of the six genes previously mapped. *AFP* and *COL1A1* showed enhanced expression during the first 4 weeks of CCl_4 treatment, but their expression declined by 8 weeks of treatment, although the expression levels remain higher than in the control (Fig. 4). This pattern is consistent with their

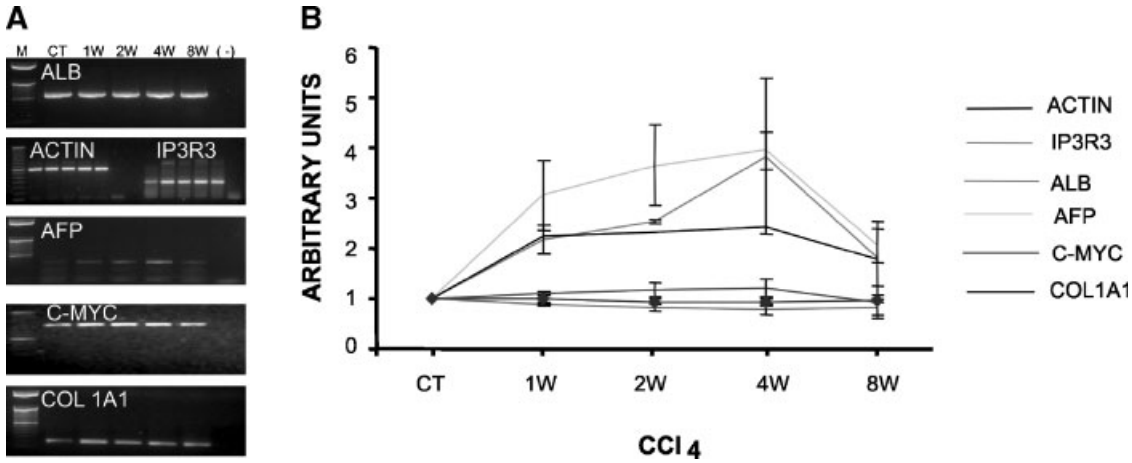

Fig. 4. Expression of the six genes positionally mapped relative to the NM, monitored by RT-PCR. **A**: The gels show the specific amplicons of the target cDNA sequences and their corresponding expression patterns following CCl_4-treatment (1, 2, 4, 8 weeks). **B**: Each time-point value in every expression curve corresponds to the average of three independent determinations in samples from different animals similarly treated.

known behavior during CCl_4-induced hepatic fibrosis [Panduro et al., 1988]. *IP3R3* that was previously reported as non-expressed in the liver based on RNA blotting [Blondel et al., 1993], nevertheless RT-PCR shows that *IP3R3* has a detectable expression in normal, control hepatocytes; a fact that was independently confirmed by another group [Martínez-Gómez and Dent, personal communication]. Moreover, in CCl_4-treated samples *IP3R3* shows a pattern similar to *AFP* and *COL1A1*: enhanced expression followed by decline but without reaching the former basal expression typical of the control (Fig. 4). It has been reported that *IP3R3* expression increases four-fold in liver homogenates of CCl_4-treated cirrhotic rats [Dufour et al., 1999], but our results indicate that *IP3R3* expression peaks and ebbs quite before the establishment of non-reversible liver cirrhosis that occurs after 12 weeks of CCl_4 treatment [Hernández-Muñoz et al., 1990]. Although the patterns of expression of *AFP*, *COL1A1*, and *IP3R3* somehow correlate with the positional changes relative to the NM observed during the induction of hepatic fibrosis (Fig. 3), other genes such as *β-actin*, *ALB*, and *c-myc* show no significant difference in their basal expression levels throughout the process of induction of hepatic fibrosis. Yet, all six genes studied show a trend to become proximal to the NM within the first 4 weeks of CCl_4 treatment, and then by 8 weeks of treatment they appear to withdraw to a distal position relative to the NM.

Positional Mapping of two Regions Within the *β-actin* Gene

Two different regions located around the middle of the *β-actin* gene but set 320 bp apart from each other (Fig. 5A) were used as targets for amplification in NM-bound templates from control and CCl_4-treated samples. The X sequence (universal actin, 254 bp in length) located closer to the 5′ end of the *β-actin* gene, amplifies in control samples digested up to 30 min with DNase I, but it is negative in samples digested for 60 min (Fig. 5B). This locates the X sequence within the 26.6–23.6% of total DNA closer to the NM according to the corresponding kinetics of nucleoid-DNA digestion (Fig. 1). However, the same sequence mapped in nucleoids from hepatocytes corresponding to 4 weeks of CCl_4 treatment, still amplifies in samples digested for 60 min (Fig. 5B), which means that the X sequence is now located within the 10.2% of total DNA closer to the NM (see the corresponding kinetics in Fig. 1). This correlates with the closest positional window relative to the NM shown by the *ALB*, *AFP*, *c-myc*, and *COL1A1* genes at 4 weeks of CCl_4 treatment (Fig. 3). On the other hand, the Y sequence (the previously mapped rat-actin amplicon of 473 bp) located closer to the 3′ end of the *β-actin* gene can be detected in samples digested up to 15 min with DNase I and thus maps in the control samples within 40.7–26.6% of total DNA closer to the NM (Figs. 1 and 5B), while in the samples corresponding to

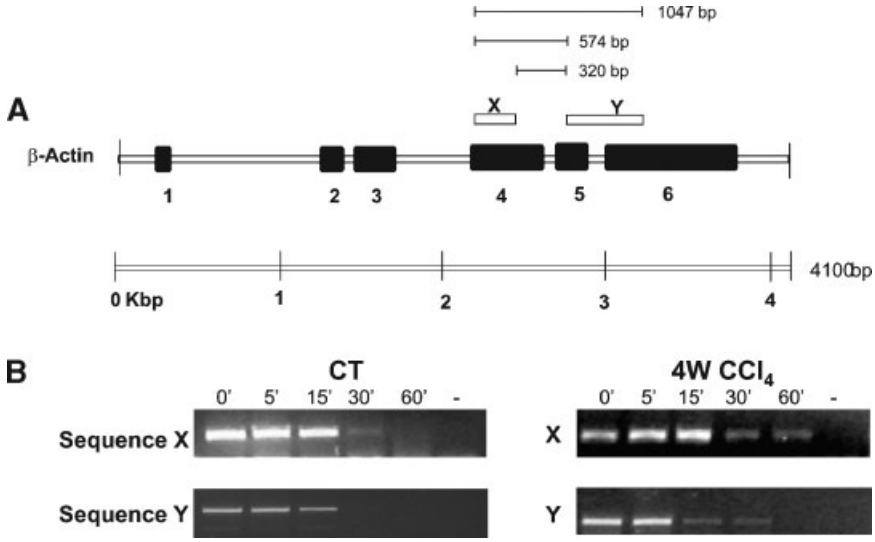

Fig. 5. Positional mapping relative to the NM of two separate regions within the *β-actin* gene. **A**: The locations of the X sequence (universal actin, 254 bp in length) and the Y sequence (rat-actin amplicon of 473 bp in length) are shown on the *β-actin* gene map. The sequences are set 320 bp apart from each other. **B**: Specific amplicons of the target sequences in nucleoids from control (CT) and 4 week CCl_4-treated hepatocytes digested for different times (0–60 min) with DNase I (0.5 U/ml).

4 weeks of CCl_4 treatment it is detected up to 30 min of DNase I digestion and so it moves to a position within 30.2–10.2% of total DNA closer to the NM (Figs. 1 and 5B). The Table I shows the percentage of nucleoid DNA at which the extinction of either the X or Y *β-actin* sequence is observed in separate control experiments. The Table II shows the percentage of nucleoid DNA at which the extinction of either the X or Y sequence is observed in separate experiments with samples corresponding to 4 weeks of CCl_4 treatment. Using data from such tables it is possible to establish separate but comparable positional windows for the X and Y sequences in either control or CCl_4-treated samples (Fig. 6A). Moreover, considering the lowest upper value and the highest lower value among the positional windows of similar experiments (see above the previously defined meaning of the upper and lower values in a positional window), it is possible to define the most-likely hypothetical positional window for either the X or Y sequence (D windows in Fig. 6A). Besides, averaging the upper and lower values of the positional windows from similar experiments and using as a calibrating gauge the corresponding average nucleoid-DNA digestion kinetics from Figure 1, it is possible to obtain an average positional window for either the X or Y sequence in control or CCl_4-treated samples (A windows in Fig. 6A). Using as an example the average positional window for the Y sequence in control samples, we graphically show how the stochastic action of DNase I upon naked, loop DNA in

TABLE I. Percentage of Nucleoid DNA at Which Extinction of the X or Y β-Actin Sequence is Observed (Control Samples)

Experiment	1			2			3			4			5		
T (min)	%	X	Y	%	X	Y	%	X	Y	%	X	Y	%	X	Y
0	100	+	+	100	+	+	100	+	+	100	N.D.	+	100	N.D.	+
5	67.8	+	+	54.9	+	+	68.2	+	+	46	N.D.	+	59	N.D.	+
15	39.2	+	+	36.6	+	+	48.7	+	+	36	N.D.	+	43	N.D.	+
30	26.6	+	−	25.6	+	−	26.8	+	−	27	N.D.	−	27	N.D.	−
60	23.4	−	−	24.2	−	−	24.3	−	−	21	N.D.	−	25	N.D.	−

Experiment numbers indicate separate control animals that were the source of the hepatocyte nucleoids. 'T' indicates the DNase I digestion time in minutes (0.5 U/ml). '%' shows the percentage of NM-bound DNA as a function of nuclease digestion time. 'X' and 'Y' refer to the corresponding amplicons of such *β-actin* gene sequences. The '+' or '−' signs indicate whether the corresponding sequence was amplified or not from the corresponding partially-digested nucleoid samples. N.D., not done.

TABLE II. Percentage of Nucleoid DNA at Which Extinction of the X or Y β-Actin Sequence is Observed (4 Weeks CCl_4-Treated Samples)

Experiment	1			2			3			4		
T (min)	%	X	Y	%	X	Y	%	X	Y	%	X	Y
0	100	+	+	100	+	+	100	+	+	100	N.D.	+
5	86.3	+	+	80	+	+	84	+	+	81.4	N.D.	+
15	44.5	+	+	55	+	+	49	+	+	35.1	N.D.	+
30	34	+	+	30.5	+	+	31.2	+	+	25.3	N.D.	−
60	11.3	+	−	8.5	+	−	9.8	+	−	11.1	N.D.	−

Experiment numbers indicate separate animals treated with CCl_4 for 4 weeks that were the source of the hepatocyte nucleoids. 'T' indicates the DNase I digestion time in minutes (0.5 U/ml). '%' shows the percentage of NM-bound DNA as a function of nuclease digestion time. 'X' and 'Y' refer to the corresponding amplicons of such *β-actin* gene sequences. The '+' or '−' signs indicate whether the corresponding sequence was amplified or not from the corresponding partially-digested nucleoid samples. N.D., not done.

time, determines the position of the Y sequence relative to the NM (Fig. 6B). It must be stressed that we are not comparing the position of sequence X with Y as if they were not part of the same gene, what we are monitoring is the movement of both sequences that belong to the same gene (*β-actin*) under two different physiological conditions (quiescence

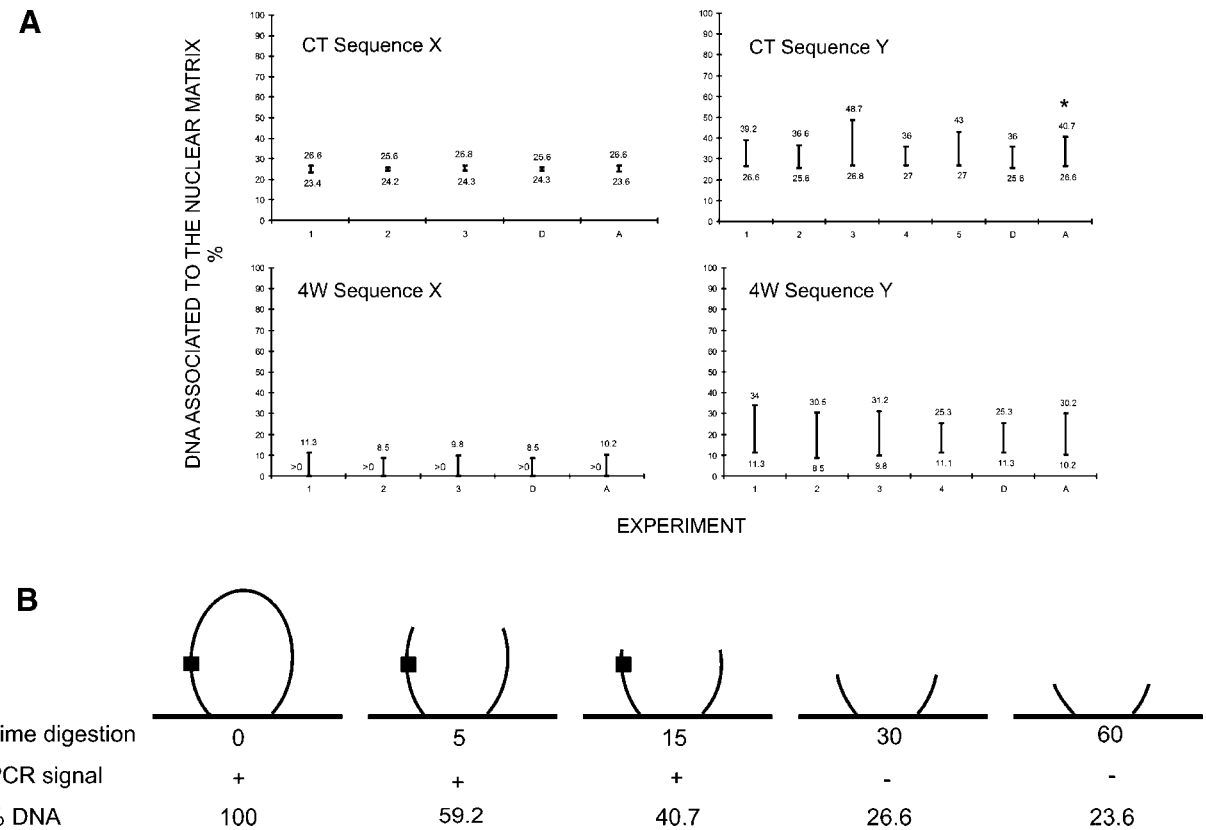

Fig. 6. Positional windows relative to the NM of the β-actin gene sequences X and Y. **A**: Positional windows established using the data from the experiments quoted in Tables I and II. The numbers in the abscissa correspond to positional windows from separate but similar mapping experiments. D = most-likely hypothetical positional window defined by considering the lowest upper value and the highest lower value among the positional windows of similar experiments. A = average positional window resulting from averaging the upper and lower values of the positional windows from similar experiments and using as calibrating gauge the corresponding average nucleoid DNA digestion kinetics from Figure 1. Positional windows lacking the lower boundary are labeled >0 to indicate that the specific gene sequence must be actually located between the specific window upper-boundary value and a greater than zero amount of residual NM-bound DNA. **B**: Drawing based on the average nucleoid DNA digestion kinetics (CT curve in Fig. 1) used for determining the average positional window for the Y sequence in control samples (*). The drawing illustrates how the stochastic action of DNase I upon naked, loop DNA in time, determines the position of the Y sequence relative to the NM, represented by the average positional window labeled with an (*) in (A) (drawing not to a scale).

and proliferation). Thus the *β-actin* gene seems to be orientated with is 5′ end towards the DNA loop anchoring point to the NM and the results suggest that the whole gene becomes closer to the NM when the hepatocytes shift from a quiescent to a proliferating state. This behavior of the *β-actin* gene during liver fibrosis induction parallels the one previously observed in hepatocytes from regenerating liver after partial hepatectomy [Maya-Mendoza et al., 2003].

DISCUSSION

Under the conditions of lysis employed to generate nucleoids, the DNA lacks the nucleosome structure because of the dissociation of histones and most other proteins usually associated with DNA; yet, the DNA loops remain topologically constrained and supercoiled but they are not organized as chromatin anymore [Cook et al., 1976; Roti-Roti et al., 1993; Aranda-Anzaldo and Dent, 1997]. Yet, such naked loop DNA is equally accessible to the endonuclease, a necessary precondition for the mapping protocol to work [Razin et al., 1995]. Moreover, some previous mapping protocols discussed elsewhere [Maya-Mendoza and Aranda-Anzaldo, 2003] used restriction enzymes for cutting the NM-attached DNA, a fact that biased the results given the sequence-specificity of such enzymes, thus ignoring the second fundamental precondition for a meaningful mapping protocol: the nuclease used for mapping the relative position of a sequence to the NM should cut all DNA sequences with equal probability [Razin et al., 1995; Razin, 2001]. It is known that DNA closest to the NM (corresponding to 1–2% of total DNA) is highly resistant to DNase I action and its average fragment length is 1.6 kb [Berezney and Buchholtz, 1981]. Indeed, two factors determine that the resistance of a given DNA sequence to DNase I is directly proportional to its proximity to the NM anchoring point: (1) steric hindrance resulting from the proteinaceous NM that acts as a barrier that relatively protects the naked loop DNA that is closer to the NM from endonuclease action [Razin et al., 1995]. (2) The loop DNA is anchored to the NM and so is topologically constrained and highly supercoiled, the degree of supercoiling being higher in the regions closer to the NM [save for the actual MARs sequences that apparently act as buffers against extreme supercoiling; Bode et al., 1992] and less intense in the distal portions of the loop. Supercoiling is a structural barrier against the action of endonucleases such as DNase I and II, that hydrolyze the DNA backbone by a single-strand cleavage (nicking) mechanism [Lewin, 1980]. Nevertheless both factors only confer relative but not absolute endonuclease-resistance to DNA and so the stochastic action of the nonspecific endonuclease implies that all sequences might be targeted to some extent at all levels of total nucleoid-DNA digestion. However, previous reports have shown that the average size of the nuclear DNA fragments liberated by nonspecific nucleases in rat hepatocytes is 0.8 kb [Berezney and Buchholtz, 1981], thus bigger than all the template sequences mapped in the present study that are <500 bp in length and so likely to be cut as whole units by the endonuclease instead of being progressively eroded by partial digestions. This fact supports our criterion of scoring the specific templates as either present (amplifiable) or absent (non-amplifiable) as a function of endonuclease-digestion time, without considering the actual intensity of the amplicon signals, since within our mapping approach it is the average relative distance to the NM anchoring point and not the actual template length the critical parameter that determines the average sensitivity to DNase I action of each sequence studied. Thus, the observed degree of resistance to DNase I digestion of a given DNA sequence corresponds to its average across the large nucleoid population analyzed. The absence of amplified product at a given digestion time-point indicates that the relative presence of the target template has fallen to a non-amplifiable level within the large nucleoid population analyzed in each sample [Maya-Mendoza and Aranda-Anzaldo, 2003; Maya-Mendoza et al., 2003]. Under our mapping scheme, the best approach for pinpointing the average position of a gene sequence relative to the NM is to increase the intermediate time-points of the DNase I digestion curves from nucleoid samples [Maya-Mendoza and Aranda-Anzaldo, 2003; Maya-Mendoza et al., 2003]. For example, the Figure 6B helps us to appreciate that the positional window for the β-actin Y sequence, corresponding to 40.7–26.6% of NM-associated DNA in nucleoids from control hepatocytes (Fig. 6A), could be eventually reduced to almost a couple of points provided that the corresponding DNase I digestion curve between 15 and 30 min includes several intermediate

digestion time-points in such a way that the precise amounts of NM-bound DNA at which the Y sequence is last amplified and then becomes non-amplifiable are determined. Thus, the specific DNA sequence corresponding to the Y amplicon is expected to be actually located within the interval defined by such values. However, given the limited number of nuclease digestion time-points of the actual nucleoid-DNA digestion curves, the positional mapping results correspond to the intervals between amounts of NM-bound DNA within which is more likely to find each specific sequence studied and such intervals only define the most probable average location relative to the NM for the specific sequences studied. Hence, our mapping approach must be regarded as semi-quantitative and topological (non-metric). In a topological space the notion of specific metrical distance between points is non-relevant and so it is dropped altogether but the neighborliness among points is crucial [Flegg, 1974], thus when measuring the relative position of points X and Y (represented by the corresponding β-actin sequences X and Y) to the reference point A (in our case represented by the attachment to the NM), the important things to consider from the topological perspective are whether X is closer to A than Y or whether Y is farther from A than X, and whether X is always between A and Y. Our results support the previously described topology, and show that the *β-actin* gene moves closer or farther from the NM as a whole unit, so if under a given circumstance Y becomes positioned between A and X then we could say that a real but forbidden transformation of the topological space (in this case defined by the nuclear substructure) has occurred.

In the case *ALB*, *AFP*, *c-myc*, and *COL1A1*, we mapped sequences corresponding to the 5′ end of such genes. The results show that in control, quiescent hepatocytes all four genes lay within a narrow positional "window" corresponding to 26.6–23.6% of the total DNA closer to the NM (Fig. 3). For *β-actin* and *IP3R3* we used sequences located somewhere from the middle to the 3′ end of such genes as targets for positional mapping relative to the NM. In quiescent hepatocytes both genes mapped within a positional window corresponding to 40.7–26.6% of the total DNA closer to the NM.

When mapping a second sequence that also belongs to the *β-actin* gene but it is located some 574 bp closer to the 5′ end of such a gene, the position of the *β-actin* gene relative to the NM shifts from 40.7–26.6% to 26.6–23.6% of total DNA closer to the NM (Figs. 1 and 5), which is basically the same positional window corresponding to the genes that were mapped using 5′-end sequences as targets. Considering that the six genes mapped are located in five different rat chromosomes and thus represent different territories or compartments within the cell nucleus [Visser and Aten, 1999; Cremer and Cremer, 2001], our results suggest that in quiescent (G0) cells most genes are located within a rather narrow positional window relative to the NM, thus supporting previous observations that suggest that most genes are located relatively close to the NM [Maya-Mendoza and Aranda-Anzaldo, 2003; Maya-Mendoza et al., 2003].

Within the first 5 weeks of CCl_4 treatment there is a progressive increase in the number of regenerating nodules in the liver, where there is intense DNA synthesis and cell proliferation [Gans and Korson, 1984; Panduro et al., 1988]. This correlates with the progressive increase in DNase I sensitivity shown by nucleoids from CCl_4-treated animals during the first 4 weeks (Fig. 1). This phenomenon has been previously described in nucleoids from other proliferating cell types [Aranda-Anzaldo, 1992, 1998], and is explained by the discontinuous model of DNA synthesis because on one side of the replication fork the DNA is single-stranded and is more easily cleaved by DNase I [Laskowski, 1971; Denhardt and Faust, 1985]. However, by the 7th week of CCl_4 treatment nodular transformation with both narrow and broad bands of fibrous stroma is widespread in the CCl_4-treated livers and the residual hepatocytes stop proliferating and significantly reduce their rate of DNA synthesis [Gans and Korson, 1984; Panduro et al., 1988; Fouad et al., 1996]. This correlates with augmented resistance to DNase I digestion shown by nucleoids from livers treated for 8 weeks with CCl_4 (Fig. 1), suggesting that global modifications in the higher-order organization of chromatin occur when the cells enter a state of permanent quiescence or replicative senescence (Fig. 3).

There is a correlation between the average size of DNA loops and the average size of replicons in different types of eukaryotic cells [Buongiorno-Nardelli et al., 1982]. In synchronized cells newly replicated DNA is bound to the NM [Aranda-Anzaldo, 1998].

Moreover, replication origins are attached to the NM [Carri et al., 1986; Dijkwel et al., 1986], and are located in or around permanent sites of DNA attachment to the NM [Razin et al., 1986; Razin, 2001]. DNA replication "factories" have been visualized as discrete foci associated with the NM [Hozák et al., 1993]. Topological considerations concerning the problems posed by tracking polymerases moving upon a structurally complex template such as DNA, support a reeling model for DNA replication according to which the DNA reels through the replication factory that extrudes newly replicated DNA [Cook, 1999]. The fact that the six genes mapped become proximal to the NM within the first 4 weeks of CCl_4 treatment, when there is widespread DNA synthesis in the regenerating liver [Gans and Korson, 1984; Panduro et al., 1988], suggest that such a movement is the result of the genes approaching or having approached the specific DNA replication sites organized upon the NM. This conclusion is supported by our previous observations that during liver regeneration after partial hepatectomy the genes become quite proximal to the NM during the main peak of DNA synthesis (that synchronously occurs in some 95% of the residual hepatocytes at 24 h post-hepatectomy) and then gradually withdraw from the NM so as to reach their original position typical of the quiescent state in control hepatocytes by day 7 post-hepatectomy [Maya-Mendoza et al., 2003].

Both *β-actin* and *IP3R3* were mapped using target sequences corresponding to their 3′-half and provide clear evidence that genes become proximal to the NM when there is significant DNA synthesis and cell proliferation, and then become distal to the NM when the cells are in the process of entering a state of either quiescence or senescence associated with non-reversible liver fibrosis (Figs. 3 and 5). Therefore, it might be the case that the further withdrawal of genes relative to the NM observed after 8 weeks of CCl_4-treatment is an early sign of permanent quiescence that correlates with the actual loss of proliferating potential in most surviving rat hepatocytes [Gans and Korson, 1984; Panduro et al., 1988; Fouad et al., 1996].

Previous reports have suggested that attachment to the NM was characteristic of active genes [Cook et al., 1982; Robinson et al., 1982; Ciejek et al., 1983; Small et al., 1985; Dalton et al., 1986; Ramana-Murty et al., 1988]. However, the RT-PCR experiments described (Fig. 4), coupled to the positional mapping results (Figs. 2 and 3), suggest that genes are positioned relative to the NM in a way that is independent of their transcriptional status or that transcription-mediated attachments to the NM, if any, are non-resistant to high-salt extraction.

Several reports indicate that chromatin moves locally as well as on a large scale within the interphase nucleus [Marshall et al., 1997; Vazquez et al., 2001; Chubb et al., 2002]. The large-scale chromatin movements in early G1 correlate with the repositioning of sub-chromosomal regions within positionally stable territories, and this includes small-scale refolding events within sub-chromosomal regions [Zink et al., 1998]. Such local chromatin movements within larger, rather stable territories might lead to DNA–protein and protein–protein interactions that mediate the attachment or detachment of DNA sequences to and from the NM. Using CCl_4 to induce hepatic fibrosis we were able to replicate a pattern of changes within the cell nucleus similar to those observed during liver regeneration after partial ablation of the liver [Maya-Mendoza et al., 2003] but in a different time scale. Different regions of each chromosome are replicated at a particular time in S phase, but on the whole genes tend to replicate earlier than non-coding DNA [Talijanidisz et al., 1989]. Thus, considering the suggestion that DNA loops correspond to replication units [Buongiorno-Nardelli et al., 1982; Djeliova et al., 2001; Razin, 2001] rearrangements in the higher-order DNA structure may affect the timing of gene replication. Indeed, CCl_4-induced hepatic fibrosis has been considered as an example of accelerated tissue-senescence resulting from repeated cycles of cell damage and regeneration [Becker, 1974], this is supported by changes in gene expression usually associated with aging [Fontoulakis et al., 2002]. Moreover, rodent cells undergo replicative senescence despite their very long telomeres and the presence of telomerase activity in somatic cells, indicating that a more general process than telomere shortening underlies cellular senescence [Campisi, 2001; Cherif et al., 2003]. Thus the modifications in topological relationships between the DNA and the nuclear substructure induced by treatment with CCl_4 might be either triggers or hallmarks of hepatocyte senescence but further experiments would be necessary to clarify this point.

ACKNOWLEDGMENTS

A. Maya-Mendoza is a CONACYT research scholar within the graduate program in Genetics and Molecular Biology at CINVESTAV-IPN. We thank Ms. L. Sánchez-Sevilla and Mr. Enrique García-Villa for technical support. We also thank Dr. M.A.R. Dent and A. Martínez-Gómez for sharing data prior to publication.

REFERENCES

Aranda-Anzaldo A. 1992. Early induction of DNA single-stranded breaks in cells infected by herpes simplex virus type 1. Arch Virol 122:317–330.

Aranda-Anzaldo A. 1998. The normal association between newly-replicated DNA and the nuclear matrix is abolished in cells infected by herpes simplex virus type 1. Res Virol 149:195–208.

Aranda-Anzaldo A, Dent MAR. 1997. Loss of DNA loop supercoiling and organization in cells infected by herpes simplex virus type 1. Res Virol 148:397–408.

Aranda-Anzaldo A, Orozco-Velasco F, García-Villa E, Gariglio P. 1999. p53 is a rate-limiting factor in the repair of higher-order DNA structure. Biochem Biophys Acta 1446:181–192.

Becker F. 1974. The liver. USA: Marcel Dekker Inc; 152p.

Berezney R, Buchholtz LA. 1981. Dynamic association of replicating DNA fragments with the nuclear matrix of regenerating liver. Exp Cell Res 132:1–13.

Berezney R, Mortillaro MJ, Ma H, Wei X, Samarabandu J. 1995. The nuclear matrix: A structural milieu for nuclear genomic function. Int Rev Cytol 162A:1–65.

Blondel O, Takeda J, Janssen H, Seino S, Graeme B. 1993. Sequence and functional characterization of a third inositol trisphospahte subtype, IP3R3, expressed in pancreatic islets, kidney, gastrointestinal tract, and other tissues. J Biol Chem 288:11356–11363.

Bode J, Kohwi Y, Dickinson L, Joh T, Klehr D, Mielke C, Kohwi-Shigematsu T. 1992. Biological significance of unwinding capability of nuclear matrix-associating DNAs. Science 255:195–197.

Buongiorno-Nardelli M, Micheli G, Carri MT, Marilley MA. 1982. A relationship between replicon size and supercoiled loop domains in the eukaryotic genome. Nature 298:100–102.

Campisi J. 2001. From cells to organism: Can we learn about aging from cells in culture? Exp Gerontol 36:607–618.

Carri MT, Micheli G, Graziano E, Pace T, Buongiorno-Nardelli M. 1986. The relationship between chromosomal origins of replication and the nuclear matrix during the cell cycle. Exp Cell Res 164:426–436.

Cherif H, Tarry JL, Ozanne SE, Hales CN. 2003. Ageing and telomeres: A study into organ- and gender-specific telomere shortening. Nucleic Acids Res 31:1576–1583.

Chubb JR, Boyle S, Perry P, Bickmore W. 2002. Chromatin motion is constrained by association with nuclear compartments in human cells. Curr Biol 12:439–445.

Ciejek EM, Tsai M-J, O'Malley BW. 1983. Actively transcribed genes are associated with the nuclear matrix. Nature 306:607–609.

Cook PR. 1999. The organization of replication and transcription. Science 284:1790–1795.

Cook PR, Brazell I, Jost E. 1976. Characterization of nuclear structures containing superhelical DNA. J Cell Sci 22:303–324.

Cook PR, Lang J, Hayday A, Lania L, Fried M, Chiswell DJ, Wyke J. 1982. Active viral genes in transformed cells lie close to the nuclear cage. EMBO J 1:447–452.

Cremer T, Cremer C. 2001. Chromosome territories, nuclear architecture and gene regulation in mammalian cells. Nat Rev Genet 2:292–300.

Dalton S, Banfield Younghusband H, Wells JRE. 1986. Chicken histone genes retain nuclear matrix association throughout the cell cycle. Nucleic Acids Res 14:6507–6523.

Denhardt DT, Faust EA. 1985. Eukaryotic DNA replication. BioEssays 2:148–153.

Dijkwel PA, Wenink PW, Poddighe J. 1986. Permanent attachment of replication origins to the nuclear matrix in BHK cells. Nucleic Acids Res 14:3241–3249.

Djeliova V, Russev G, Anachkova B. 2001. Dynamics of association of origins of DNA replication with the nuclear matrix during the cell cycle. Nucleic Acids Res 29:3181–3187.

Dufour J-F, Lüthi M, Forestier M, Magnino F. 1999. Expression of inositol 1,4,5-trisphosphate recpetor isofomrs in rat cirrhosis. Hepatology 30:1018–1026.

Ehrinpreis MN, Giambrone MA, Rojkind M. 1980. Liver proline oxidase activity and collagen synthesis in rats with cirrhosis induced by carbon tetrachloride. Biochim Biophys Acta 629:184–193.

Flegg G. 1974. From geometry to topology. London: The English University Press Ltd. pp 17–19; 156–160.

Fontoulakis M, de Vera M-C, Crameri F, Boess F, Gasser R, Albertini S, Suter L. 2002. Modulation of gene and protein expression by carbon tetracholoride in the rat liver. Toxicol Appl Pharm 183:71–80.

Fouad FM, Mamer OA, Shahidi F. 1996. Acute-phase response in rat to carbon tetrachloride-azathioprine induced cirrhosis and partial hepatectomy of cirrhotic liver. J Toxicol Environ Health 47:601–615.

Freshney I. 1994. Culture of animal cells, 3rd edn. USA: Wiley-Liss; pp 320–322.

Gans JH, Korson R. 1984. Liver nuclear DNA synthesis in mice following carbon tetrachloride administration or partial hepatectomy. Proc Soc Exp Biol Med 175:237–242.

Hernández-Muñoz R, Díaz-Muñoz M, Suárez J, Chagoya de Sánchez V. 1990. Adenosine partially prevents cirrhosis induced by carbon tetrachloride in rats. Hepatology 12: 242–248.

Hernández-Muñoz R, Díaz-Muñoz M, López V, López-Barrera F, Yáñez L, Vidrio S, Aranda-Frausto A, Chagoya de Sánchez V. 1997. Balance between oxidative damage and proliferative potential in an experimental rat model of CCl4-induced cirrhosis: Protective role of adenosine administration. Hepatology 26:1100–1110.

Hozák P, Bassim-Hassan A, Jackson DA, Cook PR. 1993. Visualization of replication factories attached to a nucleoskeleton. Cell 73:361–373.

Jackson DA, Cook PR. 1995. The structural basis of nuclear function. Int Rev Cytol 162B:125–149.

Laskowski M. 1971. In: Boyer PD, editor. The enzymes, 3rd edn. Volume IV. New York: Academic Press; 313p.

Lazarevich NL. 2000. Molecular mechanisms of alpha-fetoprotein gene expression. Biochemistry (Moscow) 65: 139–158.

Lewin B. 1980. Gene expression 2, 2nd edn. New York: John Wiley and Sons; pp 360–362.

Marshall WF, Straight A, Marko JF, Swedlow J, Dernburg A, Belmont A, Murray AW, Agard DA, Sedat JW. 1997. Interphase chromosomes undergo constrained diffusional motion in living cells. Curr Biol 7:930–939.

Maya-Mendoza A, Aranda-Anzaldo A. 2003. Positional mapping of specific DNA sequences relative to the nuclear substructure by direct polymerase chain reaction on nuclear matrix-bound templates. Anal Biochem 313: 196–207.

Maya-Mendoza A, Hernández-Muñoz R, Gariglio P, Aranda-Anzaldo A. 2003. Gene positional changes relative to the nuclear substructure correlate with the proliferating status of hepatocytes during liver regeneration. Nucleic Acids Res 31:6168–6179.

Morello D, Lavenu A, Babinet C. 1990. Differential regulation and expression of jun, c-fos and c-myc proto-oncogenes during mouse liver regeneration and after inhibition of protein synthesis. Oncogene 5:1511–1519.

Nickerson JA. 2001. Experimental observations of a nuclear matrix. J Cell Sci 114:463–474.

Panduro A, Shalaby F, Biempica L, Shafritz DA. 1988. Changes in albumin, alpha-fetoprotein and collagen gene transcription in CCl4-induced hepatic fibrosis. Hepatology 8:259–266.

Ramana-Murty CV, Mancini MA, Chatterjee B, Roy AK. 1988. Changes in transcriptional activity and matrix association of the $\alpha 2$ μ-globulin gene family in the rat liver during maturation and aging. Biochem Biophys Acta 949:27–34.

Razin SV. 2001. The nuclear matrix and chromosomal DNA loops: Is there any correlation between partitioning of the genome into loops and functional domains? Cell Mol Biol Lett 6:59–69.

Razin SV, Kekelidze MG, Lukanidin EM, Scherrer K, Georgiev GP. 1986. Replication origins are attached to the nuclear skeleton. Nucleic Acids Res 14:8189–8207.

Razin SV, Gromova II, Iarovaia OV. 1995. Specificity and functional significance of DNA interaction with the nuclear matrix: New approaches to clarify the old questions. Int Rev Cytol 162B:405–448.

Robinson SI, Nelkin BD, Vogelstein B. 1982. The ovalbumin gene is associated with the nuclear matrix of chicken oviduct cells. Cell 28:99–106.

Roti-Roti JL, Wright WD, Taylor YC. 1993. DNA loop structure and radiation response. Adv Radiat Biol 17:227–259.

Small DS, Nelkin B, Vogelstein B. 1985. The association of transcribed genes with the nuclear matrix of *Drosophila* cells during heat shock. Nucleic Acids Res 7:2413–2431.

Stein GS, van Wijnen AJ, Stein J, Lian JB, Montecino M. 1995. Contributions of nuclear architecture to transcriptional control. Int Rev Cytol 162A:251–278.

Talijanidisz J, Popowski J, Sarkar N. 1989. Temporal order of gene replication in Chinese hamster ovary cells. Mol Cell Biol 9:2881–2889.

Vazquez J, Belmont A, Sedat JW. 2001. Multiple regimes of constrained chromosome motion are regulated in the interphase *Drosophila* nucleus. Curr Biol 11:1227–1239.

Visser AE, Aten JA. 1999. Chromosomes as well as chromosomal subdomains constitute distinct units in interphase nuclei. J Cell Sci 112:3353–3360.

Zink D, Cremer T, Saffrich R, Fisher R, Trendelenburg MF, Ansorge W, Stelzer EH. 1998. Structure and dynamic of human interphase chromosome territories in vivo. Hum Genet 102:214–251.